

Turbulence Modulation Induced by Bubble Swarm in Oscillating-Grid Turbulence*

Koichi MORIKAWA**, Shigeyuki URANO**, Toshiyuki SANADA** and Takayuki SAITO**

**Department of Mechanical Engineering, Shizuoka University,
3-5-1 Johoku, Naka-ku, Hamamatsu, Shizuoka 432-8561, Japan
E-mail: ttsaito@ipc.shizuoka.ac.jp

Abstract

In the present study, liquid-phase turbulence modulation induced by a bubble swarm ascending in arbitrary turbulence was experimentally investigated. Liquid-phase homogeneous isotropic turbulence was formed using an oscillating grid in a cylindrical acrylic vessel of 149 mm in inner diameter. A bubble swarm consisting of 19 bubbles of 2.8 mm in equivalent diameter was examined; the bubble size and generating time were completely controlled using a bubble generating device through audio speakers. This bubble generating device was able to repeatedly control the bubble swarm arbitrarily and precisely. The bubble swarm was generated at a frequency of 4 Hz. The liquid phase motion was measured via two LDA (Laser Doppler Anemometer) probes. The turbulence intensity, spatial correlation and integral scale were calculated from LDA data obtained by the two spatially-separate-point measurement. When the bubble swarm was added, the turbulence intensity dramatically changed. The original isotropic turbulence was modulated to the anisotropic turbulence by the mutual interaction between the bubble swarm and the ambient isotropic turbulence. The integral scales were calculated from the spatial correlation function. The increase in turbulence intensity and the decrease in integral scale were observed by injecting the bubble swarm in oscillating-grid turbulence.

Key words: Oscillating-Grid Turbulence, Bubble Swarm, LDA, Turbulence Intensity, Spatial Correlation

1. Introduction

Gas-liquid two-phase flows are applied in many industrial plants such as GLAD system⁽¹⁾⁽²⁾. The flows are multi-scale ranging phenomena, and have complex structure. In order to operate the plants safely and efficiently, and to design optimally, a deep understanding of the flows is essentially required. The structure of the gas-liquid flows is affected by many factors: the liquid-phase parameters (e.g. vortex scale, turbulence intensity and velocity gradient), the gas-phase parameters (e.g. bubble size, number density, bubble trajectory and injection timing), and the interaction between the gas and liquid phases. It is extremely difficult to systematically clarify their turbulence structure. Although there are difficulties, the mechanism of turbulence modulation in gas-liquid two-phase flows should be experimentally and comprehensively elucidated. In addition, the experimental results and the understanding of the turbulence modulation must accelerate modeling of flows in CFD.

The conventional grid turbulence (i.e. with mean flow) has been investigated very often⁽³⁾. It was reported the decrease in the bubble rise velocity was observed in such

conventional grid turbulence⁽⁴⁾⁽⁵⁾. However, these former researches are considered to be insufficient to systematically understand the mechanism of the turbulence modulation in gas-liquid two-phase flows. In the present study, in order to extract the flow structure and the interaction between bubbles and liquid-phase motion comprehensively and systematically, we investigated liquid-phase turbulence modulation induced by the wake of a bubble swarm ascending in arbitrary turbulence. Isotropic turbulence is the most appropriate to understand the interaction between bubbles and liquid-phase turbulence. To achieve this specific purpose, we employed oscillating-grid turbulence in rest water; the oscillating grid provided conditioned homogeneous isotropic turbulence without mean flow⁽⁶⁾⁻⁽⁹⁾.

Void fraction influences the hydrodynamic interaction between gas and liquid phase⁽¹⁰⁾⁻⁽¹²⁾. Lance and Bataille⁽¹³⁾ reported that there exists a critical value of the void fraction, and the turbulent kinetic energy of the liquid may be considered to be the sum of the kinetic energy generated by the grid turbulence and that generated by bubbles below the void fraction of 1%. Therefore, the experiments should be conducted under fully controlled bubble number density and bubble size. In order to achieve these experimental conditions, the bubble swarm consisting of 19 uniform bubbles was formed and generated simultaneously under fully control of bubble diameter and formation timing through audio speakers⁽¹⁴⁾⁽¹⁵⁾ and hypodermic needles.

The liquid phase motion was measured via two LDA probes, simultaneously; the scattering noises from the bubbles were removed in data analysis. From the two spatially-separate points LDA data, turbulence intensity, spatial correlation and integral scale were calculated and discussed. From these results, we will discuss the liquid-phase turbulence modulation.

Nomenclature

- d : grid bar thickness, mm
- f : frequency of oscillating grid, Hz
- Lz : integral scale, mm
- M : mesh size, mm
- $R_{(\Delta z)}$: spatial correlation coefficient, arbitrary
- S : stroke of oscillating grid, mm
- u : horizontal velocity, m/s
- u_{rms} : root mean square of horizontal velocity, m/s
- w : vertical velocity, m/s
- w_{rms} : root mean square of vertical velocity, m/s

2. Experimental setup

The experimental setup used in the present study is illustrated in Fig. 1. The vessel was made of an acrylic pipe (149 mm in inner diameter, 600 mm in height) covered with a rectangular acrylic water jacket to eliminate refraction of laser beams. The origin of the coordinate system (x, y, z) was set at the center of the bottom of the vessel. Purified water (Deionized, filtrated tap water) was filled up to a depth of $z = 580$ mm.

We generated homogeneous isotropic turbulence in the liquid phase by oscillating a grid in rest water. The grid was tightly bolted at the end of an oscillating bar. The grid (the mesh size $M = 18$ mm, the grid bar thickness $d = 4$ mm) was oscillated by computer-controlled servomotor (frequency $f = 4$ Hz, stroke $S = 40$ mm). The neutral position of the grid was at $z = 430$ mm. The neutral grid position was redefined as new origin of z' , here z' axis was defined as downward direction.

The details of the bubble generating device are shown in Fig. 2. This device was able to form repeatedly uniform bubbles at controllable generating timing. Each audio speaker

pushed the air by fluctuation of pressure, which was sealed in a clearance between the speaker cone and acrylic box, under a well controlled pressure and flow; it formed a uniform bubble at each hypodermic needle precisely. A check valve was mounted in order to prevent the back-flow induced by oscillation of the cone. The bubble generation timing was arbitrarily controlled by the function generator; in the present experiments, it was set at 4 Hz. We used 10 audio speakers which were connected with 19 hypodermic needles (0.55 mm of outer diameter, 0.37 mm of inner diameter). These needles were able to repeatedly release bubbles at the same initial shape; in addition the trajectories were highly controlled. The average diameter of bubbles was 2.8 mm in equivalent diameter.

The liquid phase motion was measured via two one-component LDA probes (TSI IFA750). We carried out two-point simultaneous measurement in order to evaluate spatial correlations. The focal point of the master probe was fixed at $(x, z') = (0, 100)$ and $(27.5, 100)$. The focal point of the slave probe was moved from the focal point of master probe to $(x, z') = (0, 140)$ and $(27.5, 140)$ at an interval of 1 mm. We measured them at each point until obtaining 5000 data. Seeding particles were made of polystyrene particles. In general, removal of bubble-scattering noises is essential to obtain the measurement reliability when applying LDA to measurement of liquid-phase velocity in a gas-liquid two-phase flow. In this study, the bubble-scattering noises were removed by applying the same data processing as Mudde and Saito⁽¹¹⁾.

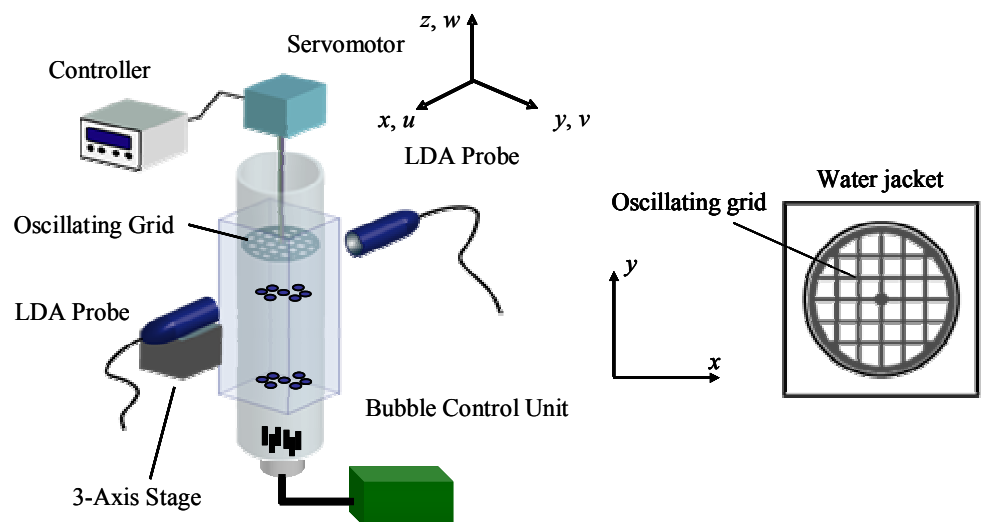


Fig. 1 Experimental setup

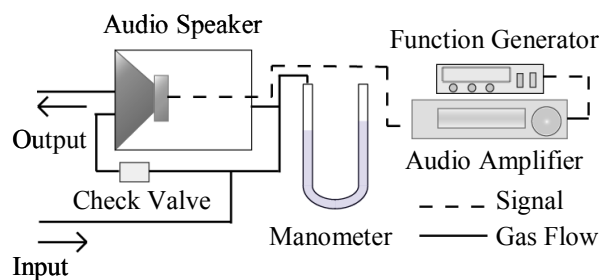


Fig. 2 Bubble Control Unit

The LDA measurements were performed under three experimental conditions, the first one was performed under the oscillating-grid turbulence without bubble swarm (hereafter Condition-O), the second one was performed under the turbulence induced by the bubble swarm in stagnant water (Condition-B), and the third one was performed under the oscillating-grid turbulence with bubble swarm (Condition-OB).

3. Experimental condition

In this study, the basic bubble shape was categorized into a type of oblate ellipsoidal⁽¹⁶⁾. The shadow images of bubbles were captured by high-speed-video camera of 1200×1632 pixels (1 pixel = 65.9 μm). The bubble images were processed to calculate the center of gravity, the major axis and minor axis. In total, 384 bubbles were analyzed, and equivalent diameter of the examined bubble was obtained as 2.8 mm. Using both hypodermic needle and audio speaker unit resulted in achievement of the high reproducibility and uniformity of the bubble size, and high controllability of bubble formation timing. Moreover, the average rise velocity of the bubbles at the center of gravity (vertical component of the bubble velocity) was obtained. Under Condition-B, the velocity was 302 mm/s at $z' = 100$ mm. Under Condition-OB, that was 301 mm/s at $z' = 100$ mm. The velocity difference between Condition-B and Condition-OB is not so large. From these results, the bubble rise velocity was considered to be hardly influenced by oscillating-grid turbulence in our experimental condition.

We measured liquid-phase velocity components w and u using a two-component-LDA probe to clarify oscillating-grid turbulence. Under Condition-O, the vertical and horizontal turbulence intensity asymptotically approached a certain value at $100 \text{ mm} \cong z'$. In this area, the flow is considered to be a homogeneous turbulence flow regardless of z' . Furthermore the ratio of the vertical to horizontal turbulence intensity (w_{rms} / u_{rms}) ranged from 0.7 to 1.3 in the area of $-40 \leq x \leq 40$ mm and $100 \leq z' \leq 180$ mm. We found out the ideal homogeneous isotropic turbulence was formed in this area. The LDA measurement is too hard to apply for bubbly flow, because the acquisition rate of accuracy velocity is dramatically decreased by scattering noise from bubble surface. Moreover many difficulties are occurred in order to achieve correct correlation coefficient of velocity. We fixed the measurement points at $x=0$ and 27.5 to eliminate huge measurement time. We could expect to observe the same turbulence modulation was occurred at measured area because of homogeneous isotropic turbulence. Hereafter, we discussed the area of $100 \leq z' \leq 130$ mm.

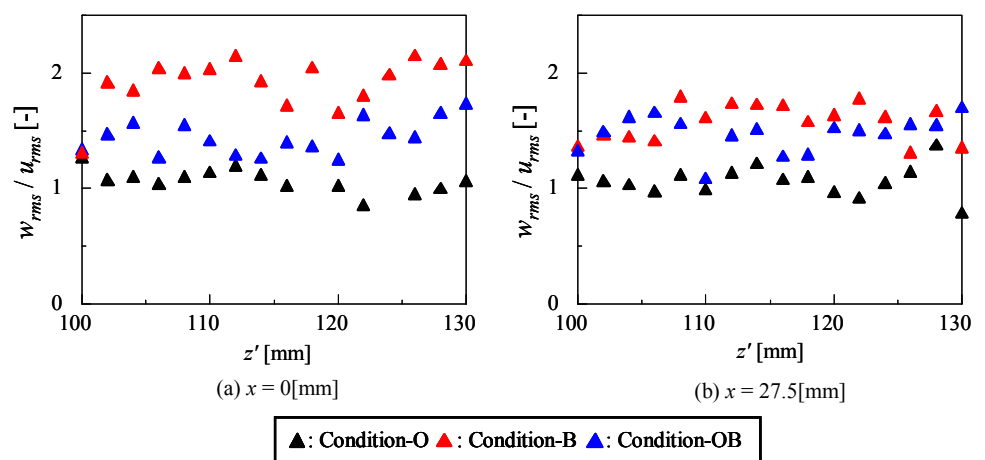


Fig. 3 Profiles of the ratio of turbulence intensity

Table 1 Average of w_{rms}/u_{rms}

	$x=0, 100 \leq z' \leq 130$	$x=27.5, 100 \leq z' \leq 130$
Condition-O	1.12	1
Condition-B	1.88	1.54
Condition-OB	1.44	1.48

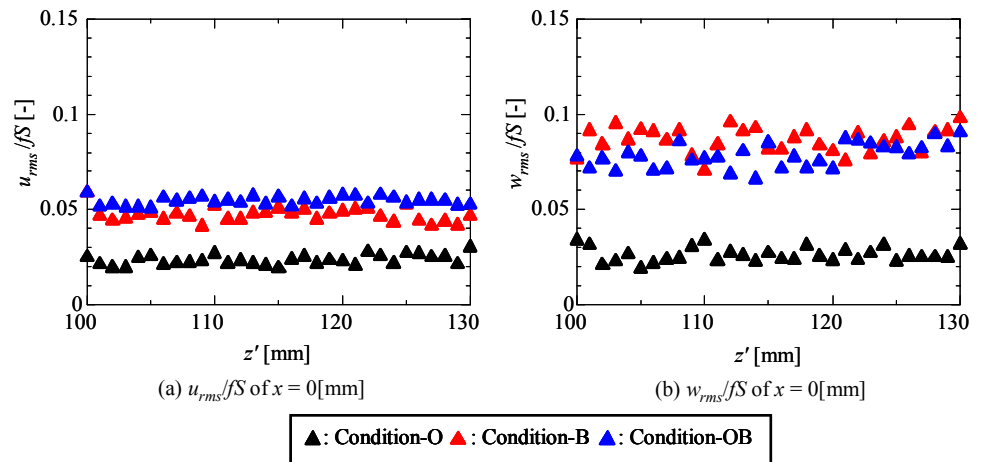


Fig. 4 Profiles of the turbulence intensity

4. Result and discussion

4. 1. Turbulence intensity

Fig. 3 shows the ratio of the vertical to horizontal turbulence intensity as a function of distance from the neutral grid position ($z' = 0$ mm). The averages of w_{rms} / u_{rms} were listed in Table 1. We found out that the homogeneous isotropic turbulence was formed in the area of $-40 \leq x \leq 40$ mm and $100 \leq z' \leq 180$ mm by oscillating grid as above. Under Condition-O, the oscillating-grid turbulence was almost isotropic (because of $w_{rms}/u_{rms} = 1$) at all measurement points. Under Condition-OB, the turbulence intensity in the vertical direction became larger than the one in the horizontal direction at all measurement points (w_{rms} is larger than u_{rms}). This indicates that the isotropic turbulence changed into anisotropic turbulence. The turbulence modulation was induced by the mutual interaction between the bubble swarm and the ambient isotropic turbulence of the liquid phase.

Fig. 4 shows the turbulence intensity ($w_{rms}/fS, u_{rms}/fS$) as a function of distance from the neutral grid position. It is clear that the values under Condition-O are smaller than those under both Condition-B and Condition-OB at all measurement points. Especially the turbulence intensity under Condition-OB was larger than that under Condition-O. Therefore we could confirm the bubble injection strongly disturbed liquid-phase turbulence.

In order to compare the turbulence intensity under Condition-B with that under Condition-OB, space-averaged turbulence intensity was calculated; the frequency and stroke of grid oscillation were applied to dimensionless expression in accordance with Hopfinger⁽⁶⁾⁽⁷⁾. The results are shown in Table 2. The space-averaged turbulence intensity of vertical velocity (w_{rms}/fS) under Condition-OB is smaller than that under Condition-B, at $x = 0$ and 27.5 mm. The turbulence intensity of the vertical velocity (w_{rms}/fS) is considered to be inhibited by the mutual interaction of the turbulence induced by the bubble swarm and the

Table 2 Space-averaged turbulence intensity

	measurement point	w_{rms}/fS [-]	u_{rms}/fS [-]
Condition-O	$x=0, 100 \leq z' \leq 130$	0.026	0.023
	$x=27.5, 100 \leq z' \leq 130$	0.020	0.020
Condition-B	$x=0, 100 \leq z' \leq 130$	0.087	0.047
	$x=27.5, 100 \leq z' \leq 130$	0.085	0.055
Condition-OB	$x=0, 100 \leq z' \leq 130$	0.078	0.054
	$x=27.5, 100 \leq z' \leq 130$	0.078	0.053

ambient isotropic turbulence. The turbulence intensity of horizontal velocity under Condition-OB is larger than that under Condition-B at $x = 0$ mm. At $x = 27.5$ mm, the turbulence intensity under Condition-OB takes almost the same value as that under Condition-B. These are also considered to be induced by the mutual interaction. Moreover, in this study, the turbulence intensity induced by bubble swarm was larger than that induced by oscillating-grid, and the turbulence intensity under Condition-OB was closer to that under Condition-B than under Condition-O. The flow was considered to be dominated by the turbulence induced by bubble swarm.

4. 2. Spatial correlation

Fig. 5 shows the spatial correlation coefficient ($R_{(\Delta z)}$) as a function of a distance (Δz) between a pair of two-probe-LDA measurement points at $x = 0$ mm. The spatial correlation coefficient was calculated by the following procedure, and plotted in Fig. 5.

$$R_{(\Delta z)} = \frac{1}{N} \sum \frac{u'(\xi) \cdot u'(\xi + \Delta z)}{u_{rms}(\xi) \cdot u_{rms}(\xi + \Delta z)} \tag{1}$$

Generally, a space correlation function is approximated by the exponential function⁽¹⁷⁾. The curves in Fig. 5 are based on the following functions.

$$R_{(\Delta z)} = Ae^{-B\Delta z^2} \tag{2}$$

$$R_{(\Delta z)} = Ae^{-C\Delta z} \tag{3}$$

In equation (2), (3), coefficient A is the value of $R_{(0)}$, namely the cross correlation at the same position. Consequently, $R_{(0)}$ should be theoretically set to unity in any conditions. The strictly simultaneous data acquisition was difficult, because the LDA measurement point has a small volume and we set the LDA measurement data within 100 μs as the simultaneous data. Therefore, the experimental results became slightly smaller than 1, though these results were reasonable; these are quite similar to past papers⁽¹⁸⁾. The solid line was drawn using equation (3); least-square approach was applied to decide the coefficient B . The broken line was also drawn using equation (2); the above method was employed. Equation (3) is more fit in the experimental data than Equation (2), in all conditions.

4. 3. Integral scale

The integral scale is defined as the following equation. The integral scale was

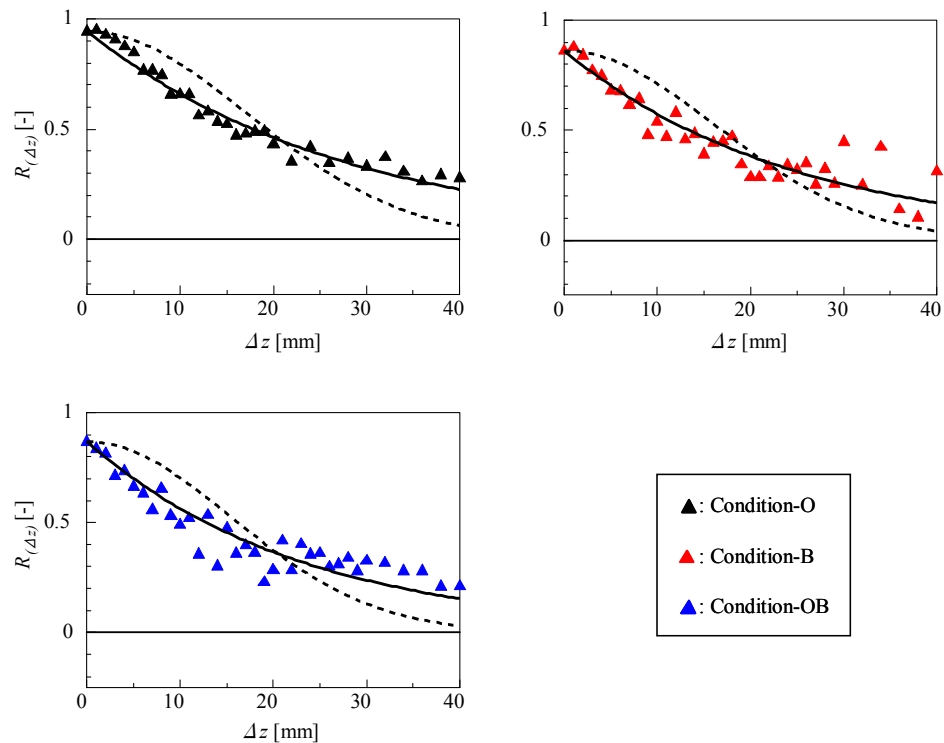


Fig. 5 Spatial correlation coefficient of w at $x = 0$ [mm]

calculated from Equation (3) (fitting in the experimental data) and Equation (4). The integral scale is measure of the size of eddies corresponding to the energy-containing range in the flow, and thus of the spatial variation of the turbulence.

$$L_z = \int_0^{\infty} R_{(\Delta z)} dz \quad (4)$$

The results of the calculation are listed in Table 3. The integral scale obtained in the present study indicates three types of tendency.

First, we could confirmed that homogeneous isotropic turbulence was formed at $x = 0$ mm under Condition-O. Generally, in homogeneous turbulence, longitudinal and transversal integral scale (calculated from longitudinal and transversal velocity correlation function) are connected that the ratio between longitudinal and transversal correlation are 2 to 1. In our study, the longitudinal velocity correlation was obtained by the velocity in same direction of LDA shifting direction, and the transversal velocity correlation was obtained by the velocity in different direction of LDA shifting direction. The ratio between longitudinal and transversal correlation became 2 to 1 (i.e. the integral scale was 26 in longitudinal direction and 13 in transversal direction), hence we could verify the ideal isotropic turbulence was formed.

Second, the significant turbulence modulation was observed. The integral scale under Condition-OB was decreased in comparison with Condition-O, though the turbulence intensity under Condition-OB was inversely increased in comparison with Condition-O. The integral scale in original isotropic turbulence was shifted to small by the injection of bubbles, and breakup of continuous liquid-phase was occurred and induced by mutual interaction between ambient liquid-phase turbulence and bubble swarm.

Third, the variance of integral scale was observed. The integral scale in respect of w under Condition-B was decreased in comparison with Condition-OB at $x = 0$ and 27.5 mm;

Table 3 Integral scale derived from spatial correlation

	x [mm]	spatial correlation	L_z [mm]
Condition-O	0	$R_{(\Delta z)}$ of u	13
		$R_{(\Delta z)}$ of w	26
	27.5	$R_{(\Delta z)}$ of u	17
		$R_{(\Delta z)}$ of w	19
Condition-B	0	$R_{(\Delta z)}$ of u	10
		$R_{(\Delta z)}$ of w	21
	27.5	$R_{(\Delta z)}$ of u	9
		$R_{(\Delta z)}$ of w	25
Condition-OB	0	$R_{(\Delta z)}$ of u	11
		$R_{(\Delta z)}$ of w	20
	27.5	$R_{(\Delta z)}$ of u	9
		$R_{(\Delta z)}$ of w	17

$L_z = 21$ and 25 mm were shifted to 20 and 17 mm, respectively. The integral scale in respect of v under Condition-B was increased in comparison with Condition-OB at $x = 0$ mm, and was the same value as the one at $x = 27.5$ mm; $L_z = 10$ mm was shifted to 11 mm, and 9 mm was retained, respectively. As discussed above, we found the decrease in turbulence intensity of the vertical component at $x = 0$ and 27.5 mm, and the increase in turbulence intensity of the horizontal component at $x = 0$ mm under Condition-OB in comparison with Condition-B. It is remarkable that correlation observed in the magnitude of the integral scale corresponds with the correlation observed in the magnitude of the turbulence intensity.

Comparing Condition-O with Condition-OB, or Condition-B with Condition-OB, the size of eddies (here, the integral scale of w) is considered to become smaller by the influence of mutual interaction between liquid-phase motion induced by bubble swarm and oscillating-grid turbulence. Therefore, in view of the integral scale, the size of eddies corresponding to the energy-containing range becomes smaller, hence it is considerable that this indicates that energy spectrum was shifted toward high wave number. However, in order to verify these opinions the measurement of the energy spectrum is needed; i.e. according to Taylor's frozen turbulence hypothesis, another LDA measurement⁽¹⁹⁾ or PIV measurement should be conducted. Besides it is necessary to more deeply understand this phenomenon on the basis of experiments on correlation between the bubble and liquid motion in different conditions. In this study, because the bubble swarm dominates liquid-phase motion (because the turbulence intensity under Condition-B was near that under Condition-OB), more experiments should be conducted in the conditions of different degree of bubble swarm domination; i.e. change of bubble diameter, bubble number density, liquid motion and so on. It is possible to clarify the mutual interaction between the bubble and liquid phases and to understand physics of the phenomenon related with the mutual interaction.

5. Conclusions

In order to clarify the structure of bubbly turbulent flows and the interaction between bubbles and liquid-phase motion, we investigated liquid-phase turbulence modulation

induced by the wake of a bubble swarm ascending in homogeneous isotropic turbulence. We utilized both oscillating-grid method and audio speaker method. From the two spatially-separate points LDA data, turbulence intensity, spatial correlation and integral scale were calculated and discussed.

When the bubble swarm was added in oscillating-grid turbulence, the turbulence intensity dramatically changed. The original isotropic turbulence was modulated to the anisotropic turbulence by the mutual interaction between the bubble swarm and ambient isotropic turbulence. The increase in turbulence intensity and the decrease in integral scale were observed by injection of bubble swarm in oscillating-grid turbulence. Comparing with turbulence induced by bubble swarm and turbulence induced by bubble swarm in oscillating-grid turbulence, the decrease in the turbulence intensity of the vertical component and the slight increase in the turbulence intensity of the horizontal component were observed. The correlation observed in the magnitude of the integral scale corresponds with the correlation observed in the magnitude of the turbulence intensity.

Acknowledgments

The present study was promoted and financially supported by Category "A" of the Grants-in-Aid for Scientific Research, Japan Society for the Promotion of Science. We thank JSPS for its help in the financial support.

References

- (1) Saito, T., Kajishima, T., Tsuchiya, K., Kosugi, S., 1999, "Mass transfer and structure of bubbly flows in a system of CO₂ disposal into the ocean by a gas lift column", *Chemical Engineering Science*, Vol. 54, pp 4945-4951
- (2) Saito, T., Kajisima, T., Nagaosa, R., 2000, "CO₂ sequestration at sea by gas-lift system of shallow injection and deep releasing", *Environ. Sci. Technol.*, Vol. 34, pp 4140-4145
- (3) Panidis, T., Papailiou, D. D., 2000, "The structure of two-phase grid turbulence in a rectangular channel: an experimental study", *Int. J. Multiphase Flow*, Vol. 26, pp 1369-1400
- (4) Poorte, R.E.G., Biesheuvel, A., 2002, "Experiments on the motion of gas bubbles in turbulence generated by an active grid", *J. Fluid Mech.*, Vol. 461, pp 127-154
- (5) Spelt, P. D. M., Biesheuvel, A., 1997, "On the motion of gas bubbles in homogeneous isotropic turbulence", *J. Fluid Mech.*, Vol. 336, pp 221-244
- (6) Hopfinger, E.J., Toly, J.-A., "Spatially decaying turbulence and its relation to mixing across density interfaces", 1976, *J. Fluid Mech.*, Vol. 78, pp 155-175
- (7) Hopfinger, E.J., Browand, F.K., Gagen, Y., 1982, "Turbulence and waves in a rotating tank", *J. Fluid Mech.*, Vol. 125, pp 505-534
- (8) Noh, Y., Fernando, H. J. S., 1995, "Onset of stratification in a mixed layer subjected to a stabilizing buoyancy flux", *J. Fluid Mech.*, Vol.304, pp 27-46
- (9) Villiermaux, E., Sixou, B., Gagne, Y., 1995, "Intense vortical structures in grid-generated turbulence", *Phys. Fluids*, Vol. 7, pp 2008-2013
- (10) Serizawa, A., Kataoka, I., Michiyoshi, I., 1975, "Turbulence structure of air-water bubbly flow", *Int. J. Multiphase Flow*, Vol. 2, pp 1415-1423
- (11) Mudde, R. F., Saito, T., 2001, "Hydrodynamical similarities between bubble column and bubbly pipe flow", *J. Fluid. Mech.*, Vol. 437, pp 203-228
- (12) Risso, F., Ellingsen, K., 2002, "Velocity fluctuations in a homogeneous dilute dispersion of high-Reynolds-number rising bubbles", *J. Fluid Mech.*, Vol. 453, pp 395-410
- (13) Lance, M., Bataille, J., 1991, "Turbulence in the liquid phase of a uniform bubbly air-water flow", *J. Fluid Mech.*, Vol. 222, pp 95-118
- (14) Kariyasaki, A., Ousaka, A., 2001, "Control of bubble size and detaching frequency from a submerged nozzle by means of pressure oscillation induced in the gas flow", *6th World*

Congress of Chemical Engineering, Melbourne, Australia

- (15) Sanada, T., Watanabe, M., Fukano, T., Kariyasaki, A., 2005, "Behavior of a single coherent gas bubble chain and surrounding liquid jet flow Structure", *Chemical Engineering Science*, Vol. 60, pp 4888–4902
- (16) Bhaga, D., Weber, M. E., 1981, "Bubbles in Viscous Liquids: Shapes, Wakes and Velocities", *J. Fluid. Mech.*, Vol. 105, pp 61-85
- (17) Belmabrouk, H., 2001, "Accuracy of Taylor length scale measurements by two-point laser Doppler velocimetry: a theoretical study", *Flow Measurement and Instrum.*, Vol. 12, pp 9-16
- (18) Nomura, T., Ishima, T., Obokata, T., 2004, "Spatial Correlation Measurements in Flow over a Rectangular Cube by Means of LDA and PIV", *Transactions of the Japan Society of Mechanical Engineers Part B (Japan)*, Vol. 689-70, pp 93-99
- (19) Sugihara, Y., Migita, M., Honji, H., 2005, "Orderly flow structures in grid-generated turbulence with background rotation", *Fluid Dynamics Research*, Vol. 36, pp 23-34